PAPER

Modeling of DS-CDMA Transmit Power Control in a Fast Fading Channel with Antenna Diversity

Akihito KATOH†, ***Student Member and*** **Fumiyuki ADACHI**†a), ***Regular Member***

SUMMARY In DS-CDMA mobile radio communications systems, transmit power control (TPC) is indispensable to regulate the variations in the received signal power produced by multipath fading. However, a practical TPC raises and lowers the mobile transmit power only at discrete time instants (the TPC rate is on the order of 1–2 kHz) and by a finite step size of the order of 1 dB. Therefore, TPC cannot completely compensate the received signal power variations and hence, the transmission performance degrades in a fast fading channel. The objective of this paper is to understand how TPC acts in a fast fading channel with antenna diversity reception and, based on this understanding, to model the TPC operation.

key words: *DS-CDMA, transmit power control, fading, mobile radio communications system*

1. Introduction

In mobile radio communications systems, the transmitted signals from different users located at different positions are received at a base station with large power difference. For direct sequence code division multiple access (DS-CDMA) mobile radio, when the power difference becomes large, large multi-access interference (MAI) occurs due to non-orthogonality among spreading codes assigned to different users. This is known as the near-far problem [1], [2]. In addition to this, according to a user's movement the received signal varies very rapidly due to shadowing and multipath fading. Shadowing and multipath fading are produced by blocking and scattering of the transmitted signal by many obstacles, located between a base station and a mobile station, respectively [3]. Multipath fading rate is much faster than shadowing. Hence, fast transmit power control (TPC) is an indispensable technique on the reverse (mobile-to-base) links of DS-CDMA mobile radio [1], [4].

DS-CDMA channel is an interference-limited channel. When TPC is used, the base station measures the instantaneous signal-to-MAI plus background noise power ratio (SINR) and sends the TPC command to each mobile station every T_{tpc} seconds (TPC command period) to raise or lower the mobile transmit power by Δ_{tpc} dB (TPC step size) [5], [6]. Since the transmit power is updated by the limited amount of Δ_{tpc} dB every T_{tpc} seconds, the fast and deep power drops due to fading cannot be fully regulated and hence the transmission performance, e.g., average bit error rate (BER) performance, may degrade compared to the ideal TPC case. In addition to TPC, antenna diversity reception is a powerful technique to reduce the fading effect. The objective of this paper is to understand how TPC acts in a fast fading channel when used together with antenna diversity and, based on this understanding, to model the TPC operation. The TPC model presented in this paper can be used to estimate the degradation of the transmission performance in a fading channel with antenna diversity.

The remainder of this paper is organized as follows. In Sect. 2, we evaluate the average BER performance with ideal TPC and practical TPC by computer simulations and discuss how the fading rate affects the BER performance achievable with TPC and antenna diversity reception. Then, based on the results obtained in Sect. 2, we model the operation of fast TPC with antenna diversity reception. Finally, in Sect. 3, we investigate the impacts of TPC parameters in a fast fading channel with antenna diversity reception. Section 4 draws some conclusions.

2. BER Performances with TPC and Antenna Diversity

It is well known that MAI can be approximated as a Gaussian process due to the central limit theorem for a large number of users. In this paper, we use this approximation [7], [8] and combine MAI with the background noise process to treat as an equivalent Gaussian process. Throughout this paper, we use the signal energy per bit-to-equivalent noise power spectrum density ratio E_b/η_0. For quaternary phase shift keying (QPSK) modulation, SINR equals $2E_b/\eta_0$. Assuming frequency non-selective Rayleigh fading channel and M-antenna diversity reception, we evaluate the average BER performances achievable with TPC and diversity reception to discuss how fading rate affects the achievable average BER performance.

2.1 Transmission System Model

Figure 1 illustrates the transmission system model.

Manuscript received January 28, 2002.
Manuscript revised August 21, 2002.

†The authors are with the Electrical and Communication Engineering, Graduate School of Engineering, Tohoku University, Sendai-shi, 980-8579 Japan.
a) E-mail: adachi@ecei.tohoku.ac.jp

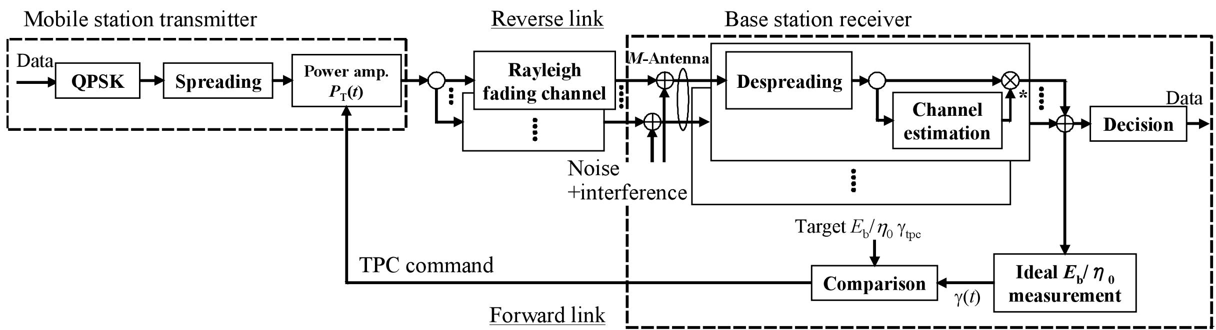

Fig. 1 Transmission system model.

Since the objective of this paper is to model the TPC operation in a fast fading channel, the effects of shadowing and distance dependent path loss are neglected. The most severe channel for DS-CDMA mobile radio is a frequency non-selective fading channel since rake combining cannot be involved. An equivalent technique to rake combining is antenna diversity reception. This paper assumes the frequency non-selective fading channel with antenna diversity using ideal maximal ratio combining (MRC) [3].

Assuming that the equivalent noise powers on all antennas are identical and represented by η_0, the instantaneous received E_b/η_0, $\gamma(t)$, at the M-antenna diversity combiner output may be expressed in continuous time representation as

$$\gamma(t) = \frac{P_T(t)T}{2\eta_0}\sum_{m=0}^{M-1} g_m(t), \tag{1}$$

where $P_T(t)$ is the mobile station transmit power, T is the QPSK symbol length in time, and $g_m(t)$ is the channel power gain associated with the mth antenna. $\{g_m(t);\ m = 0, 1, \ldots, M-1\}$ are independent identically distributed (iid) random processes. The probability density function (pdf) $p(g_m)$ and the cumulative distribution function (cdf) $P(g_m)$ of g_m are given by [3]

$$\begin{cases} p(g_m) = \exp(-g_m) \\ P(g_m) = 1 - \exp(-g_m) \end{cases}. \tag{2}$$

At the base station, the received E_b/η_0 is measured and compared to the TPC target E_b/η_0, γ_{tpc}. Assuming ideal E_b/η_0 measurement and ideal TPC, the mobile transmit power is given by

$$P_T(t) = \left(\frac{2\eta_0}{T}\right)\frac{\gamma_{tpc}}{g_{MRC}(t)}, \tag{3}$$

where

$$g_{MRC}(t) = \sum_{m=0}^{M-1} g_m(t) \tag{4}$$

is the equivalent channel power gain seen at the MRC combiner output. Equation (3) shows that the mobile transit power is inversely proportional to the equivalent channel power gain. Note that although continuous time representation is used in Eq. (3), the transmit power is updated at discrete time instants of multiples of T_{tpc} seconds by a limited amount of Δ_{tpc} dB.

2.2 Theoretical BER Performance with Ideal TPC

For ideal TPC, the received $\gamma = \gamma(t)$ is always kept at the TPC target γ_{tpc}. The BER becomes identical to the case of no fading with $\gamma = \gamma_{tpc}$, which is given by [9]

$$P_b(\gamma) = \frac{1}{2}\,erfc\sqrt{\gamma}, \tag{5}$$

where

$$erfc(x) = \frac{2}{\sqrt{\pi}}\int_x^\infty \exp(-y^2)dy.$$

On the other hand, when TPC is not employed but M-antenna diversity reception is used, the average BER $P_b(\Gamma)$ in a fading channel is given by [9]

$$P_b(\Gamma) = \frac{1}{2}\left[1 - \frac{\mu}{\sqrt{2-\mu^2}}\sum_{m=0}^{M-1}\binom{2m}{m}\left(\frac{1-\mu^2}{4-2\mu^2}\right)^m\right], \tag{6}$$

where

$$\mu = \sqrt{\frac{2(\Gamma/M)}{2(\Gamma/M)+1}} \tag{7}$$

and Γ is the total average E_b/η_0 received on M antennas. In particular, when $M = 1$ and 2, Eq. (6) becomes

$$P_b(\Gamma) = \begin{cases} \frac{1}{2}\left(1 - \sqrt{\frac{\Gamma}{\Gamma+1}}\right), & \text{for } M = 1 \\ \frac{1}{2}\left(1 - \frac{1+3/\Gamma}{(1+2/\Gamma)^{3/2}}\right), & \text{for } M = 2 \end{cases}. \tag{8}$$

2.3 BER Performance with Practical Fast TPC

Here, we investigate by computer simulations how the average BER performance with practical TPC differs

Table 1 Simulation condition.

Data modem	Modulation	QPSK
	Demodulation	Ideal coherent detection
TPC	T_{tpc}	64 symbols
	Δ_{tpc}	0.5 ~ 3dB
Propagation channel		Frequency non-selective Rayleigh fading
Antenna diversity		MRC

from that of ideal TPC. Table 1 shows the simulation conditions. We assume that $T_{tpc} = 64T$ and the fading rate is represented by the normalized maximum Doppler frequency $f_D T_{tpc}$.

Figure 2 plots the average BER performance achievable with practical TPC with $\Delta_{tpc} = 1\,\text{dB}$ as a function of the TPC target γ_{tpc} with $f_D T_{tpc}$ as a parameter. For comparison, theoretical BER performance with ideal TPC and that without TPC are also plotted (they are given by Eqs. (5) and (8)). For slow fading, i.e., $f_D T_{tpc} = 10^{-4}$, TPC can track the channel gain variations and can achieve the performance close to the ideal TPC case. The condition of $f_D T_{tpc} = 10^{-4}$ corresponds to $f_D = 0.2\,\text{Hz}$ for the QPSK symbol rate of 128 ksymbol/s. However, as fading becomes faster, the BER performance deviates from the ideal TPC case and approaches that of no TPC. When $M = 1$ and $f_D T_{tpc} = 10^{-3}$, while the BER performance remains almost the same as the ideal TPC case for $\gamma_{tpc} < 10\,\text{dB}$, it degrades significantly for $\gamma_{tpc} > 10\,\text{dB}$. It is worthwhile noting that in this large γ_{tpc} region, the BER performance curve is parallel to the no TPC case. For other values of $f_D T_{tpc}$, similar trend can be seen, e.g., when $f_D T_{tpc} = 10^{-2}$, this is seen for $\gamma_{tpc} > 7\,\text{dB}$. Also, the same is true when antenna diversity is used. The reason why the BER performance curve is parallel to the no TPC case, in large γ_{tpc} region, is discussed below.

2.4 Discussions

It can be seen from Fig. 2(a) of no antenna diversity case that the TPC target required for BER $= 10^{-4}$ is $\gamma_{tpc} = 19\,\text{dB}$ when $f_D T_{tpc} = 10^{-2}$, while the total required average received E_b/η_0 is $\Gamma = 34\,\text{dB}$ for the case of no TPC (note that this is not shown in Fig. 2(a)). That the performance curve in regions of $\gamma_{tpc} > 7\,\text{dB}$ is parallel to that of no TPC implies that the γ-variations below $\gamma < \gamma_{tpc}$ are similar to the no fading case with $\Gamma = 34\,\text{dB}$. This can be confirmed by plotting the γ-variations with and without fast TPC. Figure 3 plots an example of variations of the received E_b/η_0, γ, and the transmit E_b/η_0, γ_T, which is defined as $\gamma_T = (T/(2\eta_0))P_T$. In a time interval of $t/T = 300$ to 800, the fast TPC cannot track against the fast and deep fade and thus, the transmit power cannot be increased in inverse proportion to the channel power gain. Therefore, the received γ fades similarly in the no TPC case. This is the reason why in large γ_{tpc} regions, the BER performance curve becomes parallel to the no TPC case.

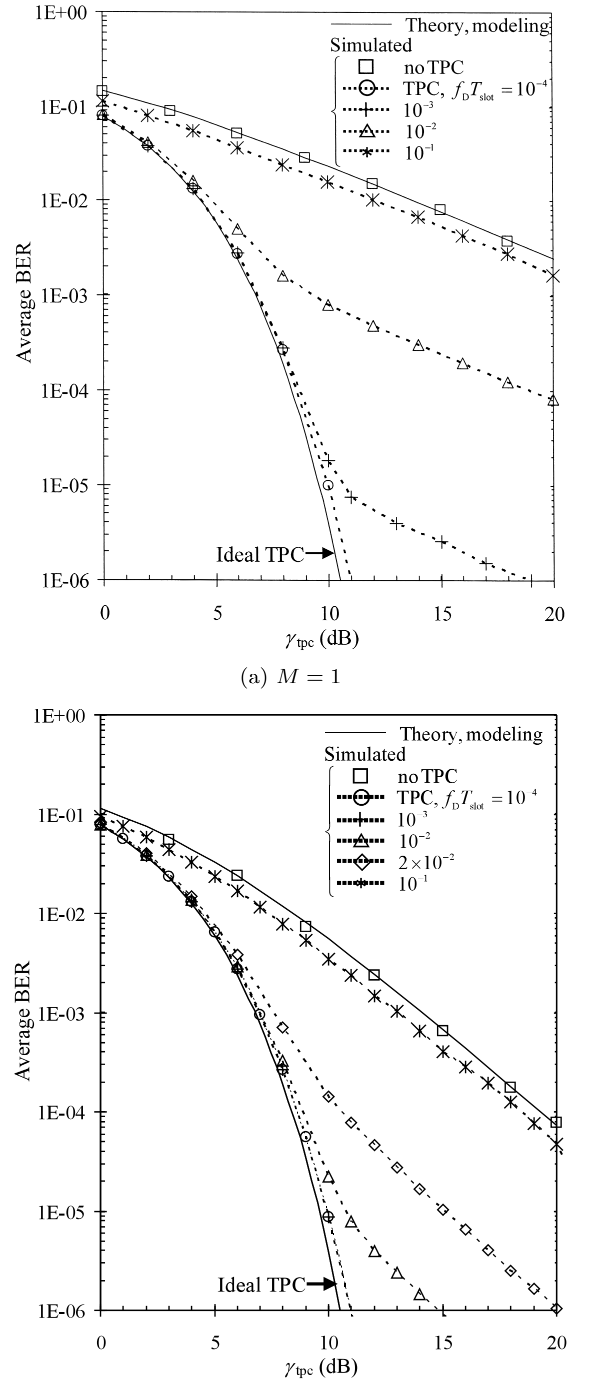

(a) $M = 1$

(b) $M = 2$

Fig. 2 Measured average BER performance when $\Delta_{tpc} = 1\,\text{dB}$.

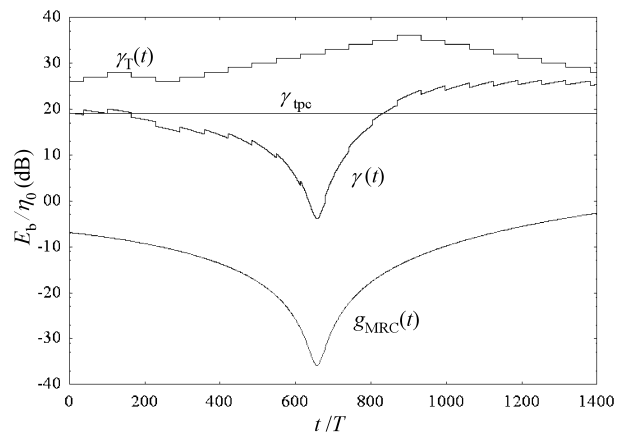

(a) TPC with $\gamma_{tpc} = 19\,\text{dB}$

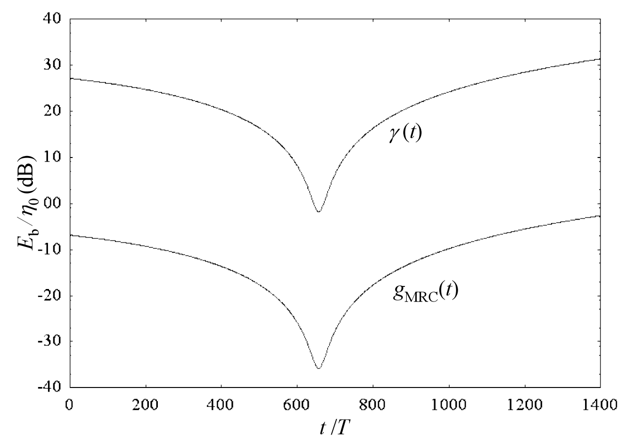

(b) no TPC with $\Gamma = 34\,\text{dB}$

Fig. 3 Variations in received γ. $f_D T_{tpc} = 0.01$ and $\Delta_{tpc} = 1\,\text{dB}$.

3. Model of Fast TPC Operation

3.1 Received E_b/η_0 Based on TPC Modeling

With ideal TPC, the transmit E_b/η_0, $\gamma_T(t)$, in the continuous time representation is given, from Eq. (3), by

$$\gamma_T(t) = P_T(t)\left(\frac{T}{2\eta_0}\right) = \frac{\gamma_{tpc}}{g_{MRC}(t)}. \tag{9}$$

However, it can be assumed from the discussion presented in Sect. 2.4 that, in a practical TPC, the transmit power cannot be increased in inverse proportion to $g_{MRC}(t)$ when the value of $g_{MRC}(t)$ falls below the threshold g_{th}. Hence, we model the time variation of transmit E_b/η_0 as follows:

$$\gamma_T(t) = \frac{\gamma_{tpc}}{\tilde{g}_{MRC}(t)}, \tag{10}$$

where $\tilde{g}_{MRC}(t)$ is the equivalent power gain given by

$$\tilde{g}_{MRC}(t) = \begin{cases} g_{MRC}(t), & \text{if } g_{MRC}(t) \geq g_{th} \\ g_{th}, & \text{otherwise} \end{cases}. \tag{11}$$

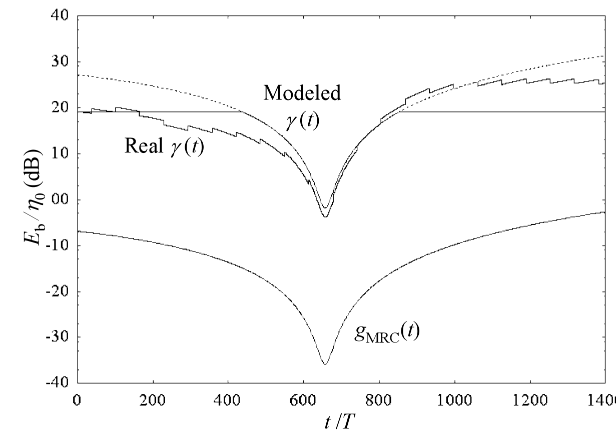

Fig. 4 Comparison of real $\gamma(t)$ and modeled $\gamma(t)$. $f_D T_{tpc} = 0.01$, $\Gamma = 34\,\text{dB}$, $M = 1$, $\Delta_{tpc} = 1\,\text{dB}$, and $\gamma_{tpc} = 19\,\text{dB}$.

Then, the resultant received E_b/η_0, $\gamma(t)$, becomes

$$\begin{aligned}\gamma(t) &= \gamma_{tpc}\frac{g_{MRC}(t)}{\tilde{g}_{MRC}(t)} \\ &= \begin{cases} \gamma_{tpc}, & \text{if } g_{MRC}(t) \geq g_{th} \\ \left(\dfrac{\gamma_{tpc}}{g_{th}}\right) g_{MRC}(t), & \text{otherwise} \end{cases},\end{aligned} \tag{12}$$

which means that $\gamma(t)$ varies in proportion to the real channel gain when $\gamma(t) < \gamma_{tpc}$. Remember that most of the decision errors are produced when $\gamma(t)$ falls close to the noise power. This means that the resultant average BER performance becomes parallel to the no TPC case in high γ_{tpc} regions. Hence, from Eq. (12), the time variation of $\gamma(t)$ with practical TPC can be viewed as the one without TPC having the average E_b/η_0 Γ, given by

$$\Gamma = \left(\frac{\gamma_{tpc}}{g_{th}}\right) E[g_{MRC}(t)] = M\frac{\gamma_{tpc}}{g_{th}}. \tag{13}$$

The above TPC operation modeling is applied to obtain the variations in $\gamma(t)$ of the practical TPC in fast fading with $f_D T_{tpc} = 0.01$. The value of g_{th} can be found by comparing the measured BER performance of TPC with that of no TPC. We choose, from Fig. 2, a certain value of target TPC γ^*_{tpc} in the region where the measured average BER performance curve is parallel to that of no TPC. Then, we find the value of Γ^* for no TPC that gives the same average BER. Finally, g_{th} can be obtained from

$$g_{th} = M\frac{\gamma^*_{tpc}}{\Gamma^*}. \tag{14}$$

The value of g_{th} for $M = 1$ was found to be $-15\,\text{dB}$ and the real $\gamma(t)$ and the modeled $\gamma(t)$ are compared in Fig. 4. A good agreement is seen in the regions of $\gamma(t) < \gamma_{tpc}$.

Figure 5 plots the cdf's of γ as a function of the relative received E_b/η_0, γ/γ_{tpc}, for various values of

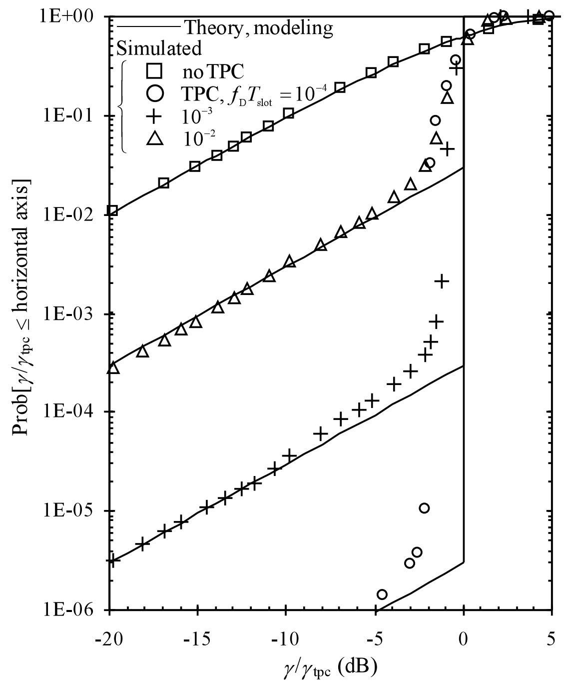

(a) $M = 1$

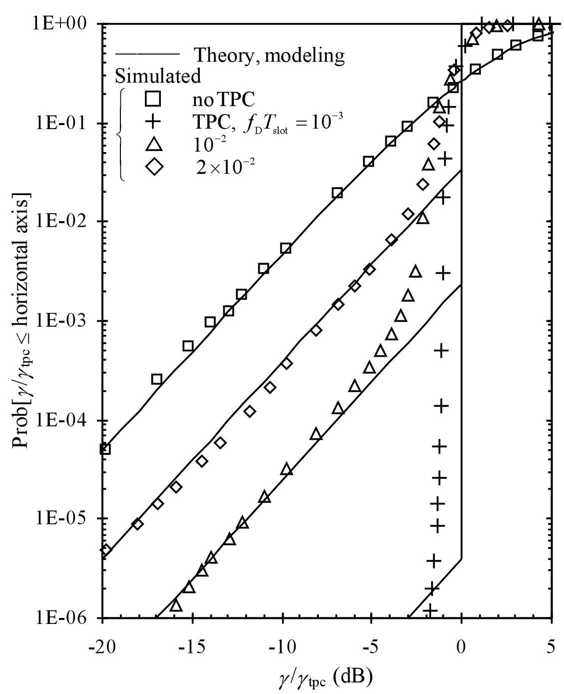

(b) $M = 2$

Fig. 5 Comparison of measured cdf of γ and that obtained theoretically based on TPC modeling. $\Delta_{tpc} = 1\,\text{dB}$.

$f_D T_{tpc}$, when $\Delta_{tpc} = 1\,\text{dB}$ to compare the measured cdf of γ and that obtained theoretically based on TPC modeling. Applying the model of Eq. (12), the theoretical cdf of γ is given by

$$P(\gamma)=\begin{cases}1-\exp\left(-\dfrac{\gamma}{\gamma_{tpc}/g_{th}}\right)\displaystyle\sum_{m=0}^{M-1}\dfrac{\{\gamma/(\gamma_{tpc}/g_{th})\}^m}{m!}, \\ \quad \text{if} \quad \gamma < \gamma_{tpc} \\ 1, \quad \text{otherwise.}\end{cases} \tag{15}$$

With no TPC, it is given by [3]

$$P(\gamma) = 1 - \exp\left(-\frac{\gamma}{\Gamma}\right)\sum_{m=0}^{M-1}\frac{(\gamma/\Gamma)^m}{m!}. \tag{16}$$

It can be clearly seen from Fig. 5 that the measured cdf and the one obtained theoretically based on TPC modeling show good agreement if $\gamma/\gamma_{tpc} < -5\,\text{dB}$.

The value of g_{th} depends on the values of $f_D T_{tpc}$, M and Δ_{tpc} and was found using Eq. (14) by comparing the measured BER performance of TPC with that of no TPC for various values of $f_D T_{tpc}$ and M when $\Delta_{tpc} = 1\,\text{dB}$. The results are plotted in Fig. 6 for $M = 1$ and 2, from which the following relationship can be found for $f_D T_{tpc} < 0.02$:

$$g_{th} = c(M, \Delta_{tpc})(f_D T_{tpc})^2 \tag{17}$$

where $c(M, \Delta_{tpc})$ is a function of M and Δ_{tpc}. Equation (17) is confirmed by the theory in Appendix, but $c(M, \Delta_{tpc})$ needs to be estimated based on the computer simulations. Using computer simulation results and Eq. (14), we found that $c(M, \Delta_{tpc} = 1\,\text{dB}) = 3.0 \times 10^2$ and 7.2×10^2 for $M = 1$ and 2, respectively. Also plotted in Fig. 6 is the measured normalized fade duration $\bar{\tau}/T_{tpc}$ at $g_{MRC}(t) = g_{th}$. The solid lines in the figure are the estimated $\bar{\tau}/T_{tpc}$ curves based on TPC modeling. They are computed using Eq. (A·8) of Appendix. For this computation, it is necessary to find δ_{th}. It was found from Eq. (A·5) that $\delta_{th} \approx 1.8\,\text{dB}$ and $1.2\,\text{dB}$ and thus, $\bar{\tau}/T_{tpc} = 6.9$ and 5.3 for $M = 1$ and 2, respectively. Fairly good agreement between the measured and estimated fade duration curves is seen.

Table 2 shows the value of $c(M, \Delta_{tpc})$ for various values of M and Δ_{tpc}. Also shown are the values of δ_{th}/T_{tpc} and $\bar{\tau}/T_{tpc}$. For the given M, as the step size Δ_{tpc} becomes larger, $c(M, \Delta_{tpc})$ decreases (i.e., δ_{th} increases) since the tracking ability of TPC against fading improves. On the other hand, for the given Δ_{tpc}, as the number M of antennas increases, $c(M, \Delta_{tpc})$ increases (i.e., δ_{th} decreases). A possible reason for this may be that the variations of $g_{MRC}(t)$ becomes less severe as M increases.

3.2 BER Analysis Based on TPC Modeling

The average BER $P_b(\gamma_{tpc})$ for coherent QPSK can be computed from

$$P_b(\gamma_{tpc}) = \frac{1}{2}\int_0^\infty erfc\sqrt{\gamma}p(\gamma)d\gamma, \tag{18}$$

where $p(\gamma)$ is the pdf of γ and can be obtained from

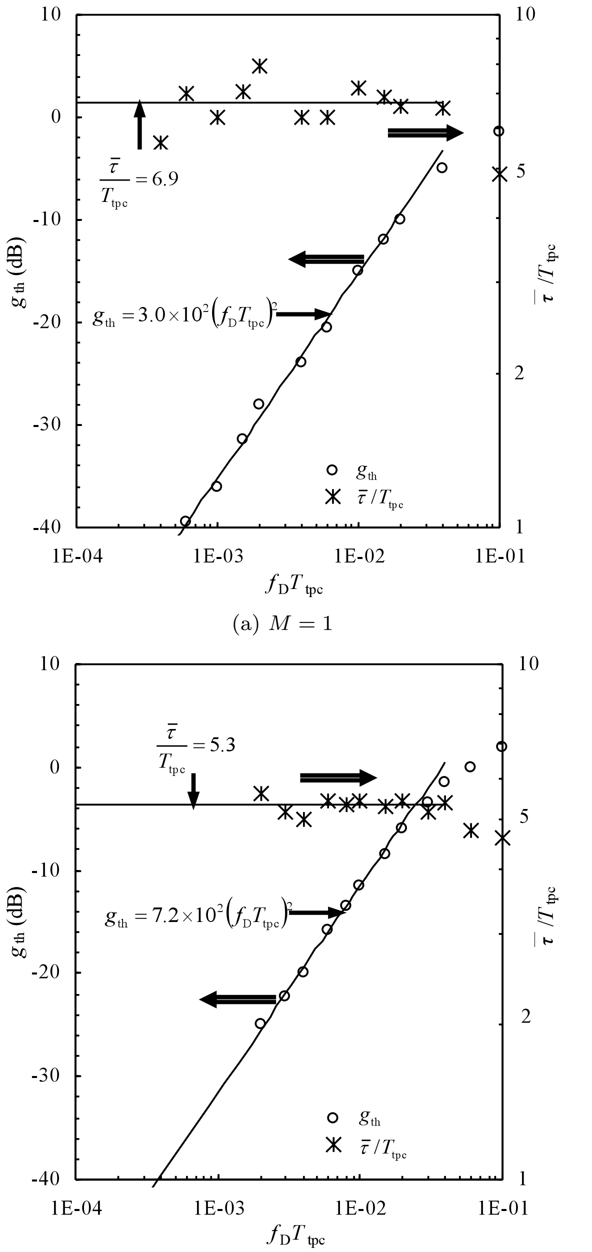

(a) $M = 1$

(b) $M = 2$

Fig. 6 Measured value of g_{th} and normalized fade duration $\bar{\tau}/T_{tpc}$ when $\Delta_{tpc} = 1$ dB.

Eqs. (15) and (16). When $M \geq 1$, substituting

$$p(\gamma) = \begin{cases} \dfrac{\gamma^{M-1}}{(\gamma_{tpc}/g_{th})^M} \exp\left(-\dfrac{\gamma}{\gamma_{tpc}/g_{th}}\right), \\ \quad \text{if} \quad \gamma < \gamma_{tpc} \\ \exp(-g_{th})\delta(\gamma - \gamma_{tpc}) \displaystyle\sum_{m=0}^{M-1} \frac{g_{th}^m}{m!}, \\ \quad \text{otherwise} \end{cases} \tag{19}$$

into Eq. (18), we have

Table 2 Measured values of $c(M, \Delta_{tpc})$, δ_{th}, and $\bar{\tau}/T_{tpc}$.

(a) Effect of M

M	$c(M, \Delta_{tpc}$=1dB)	δ_{th} (dB)	$\bar{\tau}/T_{tpc}$
1	3.0×10^2	1.8	6.9
2	7.2×10^2	1.2	5.3
3	1.0×10^3	9.6×10^{-1}	4.3
4	1.5×10^3	8.0×10^{-1}	3.8

(b) Effect of Δ_{tpc}

M	Δ_{tpc}(dB)	$c(M, \Delta_{tpc})$	δ_{th} (dB)	$\bar{\tau}/T_{tpc}$
1	0.5	1.0×10^3	9.7×10^{-1}	1.3×10^1
	1.0	3.0×10^2	1.8	6.9
	1.5	1.5×10^2	2.5	4.9
	2.0	1.1×10^2	3.0	4.1
	3.0	5.4×10^1	4.2	2.9
2	0.5	2.1×10^3	6.7×10^{-1}	9.2
	1.0	7.2×10^2	1.2	5.3
	1.5	4.2×10^2	1.5	4.1
	2.0	2.9×10^2	1.8	3.4
	3.0	1.8×10^2	2.3	2.7

$$\begin{aligned} P_b(\gamma_{tpc}) = \frac{1}{2}\Bigg[1 - &\frac{1 - erfc\sqrt{\gamma_{tpc} + g_{th}}}{\sqrt{1 + g_{th}/\gamma_{tpc}}} \sum_{m=0}^{M-1} \binom{2m}{m} \\ &\cdot \frac{1}{\{4(1 + \gamma_{tpc}/g_{th})\}^m}\Bigg] \\ &+ \sqrt{\frac{\gamma_{tpc}}{\pi}} \exp\{-(\gamma_{tpc} + g_{th})\} \\ &\cdot \sum_{m=1}^{M-1} \binom{2m}{m} \frac{1}{\{4(1 + \gamma_{tpc}/g_{th})\}^m} \\ &\cdot \sum_{n=0}^{m-1} \frac{\{2(\gamma_{tpc} + g_{th})\}^n}{(2n+1)!!}. \end{aligned} \tag{20}$$

Note that when $M = 1$, $\sum_{m=1}^{0}(.) = 0$ in Eq. (20). Substituting the values of g_{th}, obtained from computer simulation, into Eq. (20), the theoretical BER performance based TPC modeling can be obtained and the results are plotted in Fig. 7. Also plotted is the measured BER performance of the practical TPC. Fairly good agreement is seen. This confirms the validity of our TPC modeling.

4. Conclusion

In this paper, practical TPC in a fast fading channel with M-antenna MRC diversity was modeled. In this model, when the equivalent channel power gain, $g_{MRC}(t)$, seen at diversity combiner output falls below a threshold value, g_{th}, the fast TPC cannot track against channel power gain variation. The parameter of

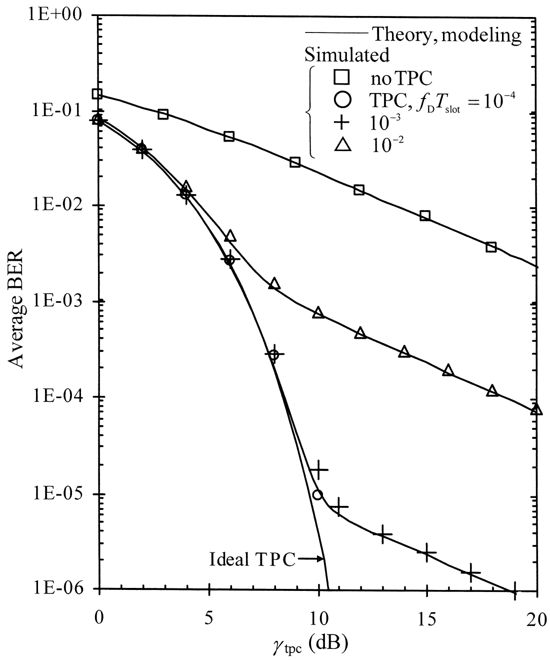

(a) $M = 1$

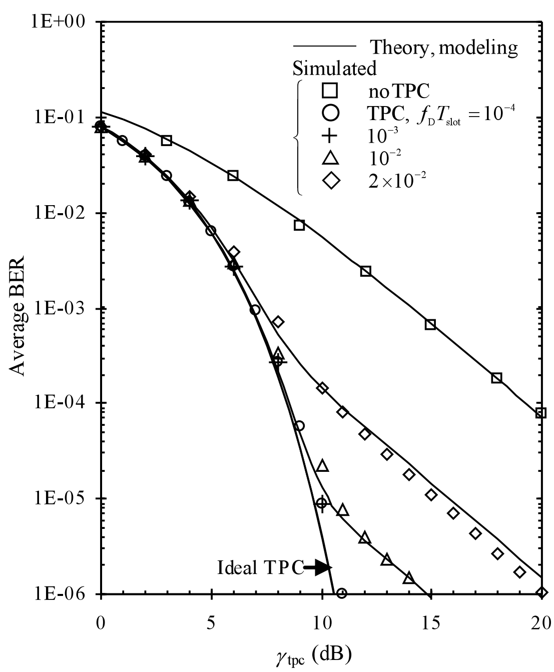

(b) $M = 2$

Fig. 7 Comparison of theoretical BER performance based on TPC modeling and measured BER performance when $\Delta_{tpc} = 1$ dB.

this TPC modeling is g_{th}, which depends on $f_D T_{tpc}$, M and Δ_{tpc}. It was theoretically found that g_{th} is proportional to $(f_D T_{tpc})^2$. The dependence of g_{th} and $\bar{\tau}/T_{tpc}$ on M and Δ_{tpc} was determined by computer simulations. Then, the cdf of the E_b/η_0, γ, and the average BER performance were estimated and compared with measured results to find fairly good agreement. TPC modeling presented in this paper can be used to understand the TPC operation in a fast fading channel and to estimate the degradation of transmission performance. The understanding of fade duration with fast TPC may contribute to better designing of an error control system with fast TPC and antenna diversity reception in a fading channel.

References

[1] A.J. Viterbi, CDMA: Principles of spread spectrum communications, Addison-Wesley, 1995.

[2] R. Kohno, R. Meiden, and L. Milstein, "Spread spectrum access methods for wireless communications," IEEE Commun. Mag., vol.33, no.1, pp.58–67, Jan. 1995.

[3] W.C. Jakes, Jr., ed., Microwave mobile communications, Wiley, New York, 1974.

[4] K. Gilhausen, I.M. Jacobs, A.J. Viterbi, L.A. Weaver, and C.E. Wheatley, III, "On the capacity of a cellular CDMA system," IEEE Trans. Veh. Technol., vol.40, pp.303–312, May 1991.

[5] S. Ariyavistakul, "Signal and interference statistics of a CDMA system with feedback power control—Part II," IEEE Trans. Commun., vol.42, no.2/3/4, pp.597–605, Feb./March/April 1994.

[6] S. Seo, T. Dohi, and F. Adachi, "SIR-based transmit power control of reverse link for coherent DS-CDMA mobile radio," IEICE Trans. Commun., vol.E81-B, no.7, pp.1508–1516, July 1998.

[7] C. Kchao and G.L. Stuber, "Analysis of a direct-sequence spread-spectrum cellular radio system," IEEE Trans. Commun., vol.41, no.10, pp.1507–1516, Oct. 1993.

[8] F. Adachi, K. Ohno, A. Higashi, T. Dohi, and Y. Okumura, "Coherent multicode DS-CDMA mobile radio access," IEICE Trans. Commun., vol.E79-B, no.9, pp.1316–1325, Sept. 1996.

[9] J.G. Proakis, Digital Communications, 3rd ed., McGraw-Hill, New York, 1995.

[10] Y. Okumura and M. Shinji, ed., Fundamentals of mobile communications, IEICE, 1986.

Appendix

The equivalent channel power gain with M-antenna MRC antenna diversity $g_{MRC}(t) = \sum_{m=0}^{M-1} g_m(t)$ is expressed in dB. Let $g_m(t) = r_m^2(t)$, where $r_m(t)$ is a random process following Rayleigh distribution. The time derivative of $\chi(t) = 10\log_{10}[g_{MRC}(t)]$ at $g_{MRC}(t) = g_{MRC}$ is given by

$$\chi = \frac{20}{\ln 10}\frac{1}{g_{MRC}}\sum_{m=0}^{M-1} r_m r_m' \text{ dB/sec}, \qquad (\text{A}\cdot 1)$$

where $r_m' = r_m'(t) = dr_m(t)/dt$. According to TPC modeling presented in this paper, the fast TPC cannot track against $g_{MRC}(t)$ when $g_{MRC}(t) < g_{th}$. We assume that the value of g_{th} is the level that gives $E[|\chi|] = \delta_{th}$ dB per T_{tpc} sec, where $E[.]$ represents ensemble average operation.

In Rayleigh fading, $\{r_m';\ m = 0, 1, \ldots, M-1\}$ are the random variables which follow iid Gaussian distributions with zero mean and equal variance of $2(\pi f_D)^2$. Hence, for the given $\{r_m;\ m = 0, 1, \cdots, M-1\}$, χ becomes zero-mean Gaussian variable. Since $g_{MRC} = \sum_{m=0}^{M-1} r_m^2$, the variance of χ is given by

$$\sigma^2 = E[\chi^2] = \left(\frac{20}{\ln 10}\right)^2 \frac{1}{g_{MRC}^2} \sum_{m=0}^{M-1} r_m^2 E[{r_m'}^2]$$
$$= \left(\frac{20}{\ln 10}\right)^2 2(\pi f_D)^2 \frac{1}{g_{MRC}^2} \sum_{m=0}^{M-1} r_m^2$$
$$= \left(\frac{20}{\ln 10}\right)^2 \frac{2(\pi f_D)^2}{g_{MRC}}. \qquad (\text{A}\cdot 2)$$

Therefore, $E[|\chi|]$ becomes

$$E[|\chi|] = \sqrt{\frac{2}{\pi}}\sigma = \frac{20}{\ln 10}\frac{2 f_D\sqrt{\pi}}{\sqrt{g_{MRC}}}. \qquad (\text{A}\cdot 3)$$

Letting $g_{MRC} = g_{th}$ and equating $E[|\chi|]$ to δ_{th}/T_{tpc}, g_{th} is obtained as

$$g_{th} = c(M, \Delta_{tpc})(f_D T_{tpc})^2, \qquad (\text{A}\cdot 4)$$

where

$$c(M, \Delta_{tpc}) = \left(\frac{20}{\ln 10}\frac{2\sqrt{\pi}}{\delta_{th}}\right)^2, \qquad (\text{A}\cdot 5)$$

which is Eq. (17). The value of g_{th} is found by comparing the measured BER performance of TPC and that of no TPC and using Eq. (14). Then, once $c(M, \Delta_{tpc})$ is found, δ_{th} can be obtained using Eq. (A·5) for the given $f_D T_{tpc}$.

We may be interested in the average fade duration $\bar{\tau}$ of $g_{MRC}(t)$ at $g_{MRC} = g_{th}$. The average fade duration normalized by the TPC period T_{tpc} can be obtained as [10]

$$\frac{\bar{\tau}}{T_{tpc}} = \frac{f_D\bar{\tau}}{f_D T_{tpc}}$$
$$= \frac{(M-1)!}{f_D T_{tpc}} \frac{\exp(g_{th}) - \sum_{m=0}^{M-1} g_{th}^m/m!}{\sqrt{2\pi} g_{th}^{M-1/2}}$$
$$= \frac{(M-1)!}{f_D T_{tpc}} \frac{\sum_{m=M}^{\infty} g_{th}^m/m!}{\sqrt{2\pi} g_{th}^{M-1/2}}. \qquad (\text{A}\cdot 6)$$

When $g_{th} \ll 1$, Eq. (A·6) can be well approximated as

$$\frac{\bar{\tau}}{T_{tpc}} \approx \frac{1}{M}\frac{\sqrt{g_{th}}}{\sqrt{2\pi} f_D T_{tpc}}. \qquad (\text{A}\cdot 7)$$

Finally, substitution of Eqs. (A·4) and (A·5) into Eq. (A·7) gives

$$\frac{\bar{\tau}}{T_{tpc}} \approx \frac{20\sqrt{2}}{M \ln 10}\frac{1}{\delta_{th}}. \qquad (\text{A}\cdot 8)$$

Akihito Katoh received his B.S. degree in communications engineering from Tohoku University, Sendai, Japan, in 2001. Currently, he is a graduate student at the Department of Electrical and Communications Engineering, Tohoku University. His research interests include the theoretical aspects of transmit and receive diversity and transmit power control in the cellular mobile communications systems.

Fumiyuki Adachi received his B.S. and Dr.Eng. degrees in electrical engineering from Tohoku University, Sendai, Japan, in 1973 and 1984, respectively. In April 1973, he joined the Electrical Communications Laboratories of Nippon Telegraph & Telephone Corporation (now NTT) and conducted various types of research related to digital cellular mobile communications. From July 1992 to December 1999, he was with NTT Mobile Communications Network, Inc. (now NTT DoCoMo, Inc.), where he led a research group on wideband/broadband CDMA wireless access for IMT-2000 and beyond. Since January 2000, he has been with Tohoku University, Sendai, Japan, where he is a Professor of Electrical and Communication Engineering at Graduate School of Engineering. His research interests are in CDMA and TDMA wireless access techniques, CDMA spreading code design, Rake receiver, transmit/receive antenna diversity, adaptive antenna array, bandwidth-efficient digital modulation, and channel coding, with particular application to broadband wireless communications systems. From October 1984 to September 1985, he was a United Kingdom SERC Visiting Research Fellow in the Department of Electrical Engineering and Electronics at Liverpool University. From April 1997 to March 2000, he was a visiting Professor at Nara Institute of Science and Technology, Japan. He was a co-recipient of the IEICE Transactions best paper of the year award 1996 and again 1998. He is an IEEE Fellow and was a co-recipient of the IEEE Vehicular Technology Transactions best paper of the year award 1980 and again 1990 and also a recipient of Avant Garde award 2000.